Composites Part B 177 (2019) 107460

Contents lists available at ScienceDirect

Composites Part B

journal homepage: www.elsevier.com/locate/compositesb

Non-destructive testing for carbon-fiber-reinforced plastic (CFRP) using a novel eddy current probe

Dehui Wu, Fang Cheng *, Fan Yang, Chao Huang

Department of Electronic Mechanical Engineering, School of Aerospace Engineering, Xiamen University, Fujian Xiamen, 361005, China

ARTICLE INFO

Keywords:
Carbon fiber reinforced plastics (CFRP)
Eddy current testing (ECT)
Defects
8-Shaped coil
In-plane waviness
Fiber orientation

ABSTRACT

Carbon-fiber-reinforced plastic (CFRP) is of low conductivity and has a layered structure. High-frequency transmitter-receiver (T-R) probes are widely chosen to inspect CFRPs using eddy current testing (ECT). However, in these works, the variation in the distance between the probe and test sample can cause a larger signal than that caused by defects and may cover up the defect. The detection sensitivity was also reduced by random noise resulting from lift-off change. To address these issues, it is meaningful to design a probe which can overcome the effect of lift-off variation and meanwhile offer high sensitivity to defects in CFRPs. In this study, a T-R probe with a special structure for detection of CFRPs was developed. The probe contains an 8-shaped transmitter coil (TX coil) and a circular receiver coil (RX coil), which is placed on a line equidistant from the two parts of the transmitter coil. Theoretically, regardless of how the lift-off changes, the output signal is always 0 if the azimuth of the probe agrees with one of the fiber orientations of an intact CFRP. Experimental studies demonstrate that the proposed probe is insensitive to lift-off compared with a traditional T-R probe and offers high sensitivity to defects. For defect detection, in-plane waviness can be detected with the proposed probe. Quantitative experiments for crack detection were performed. The cracks were clearly visualized in the scanning images. The length and location of the cracks can also be estimated from the scanning images.

1. Introduction

Carbon fiber reinforced plastic (CFRP) is becoming more and more important in many lightweight applications ranging from aerospace to automobile manufacturing [1,2]. Hidden defects that arise during production, may lead to subsequent quality problems, and result in increased costs and risks. Typical defects during production are fiber misalignment, missing bundles, wrinkles. During use, CFRP laminates are prone to cracks, delamination, and impact damages [2]. To guarantee quality and reliability, many non-destructive testing methods have been developed to inspect CFRPs, including eddy current testing [3], ultra-sonic testing [4], X-ray [5], acoustic emission [6], infrared thermography (IRT) [7–10]. The selection of inspection method is based on the specific engineering application.

ECT is a widely used nondestructive testing (NDT) method based on electromagnetic principles. It is a fast, noncontact and real-real time NDT technique for the detection of defects which may cause conductivity and permeability variations. Defects in CFRP may change the Fiber/Volume Ratio, also resulting in variation in local average conductivity of the material, and a change of electrical connection characteristics between fiber bundles and the dielectric properties of the matrix material. Those changes in electrical characteristics can be detected by ECT scanning technology.

ECT is suitable for detecting many types of defects in thin layer CFRP structures, such as fiber misalignment, cracks, delamination and in-plane waviness [2]. The detection coil has a great impact on the performance of the eddy current testing system. Some studies on the detection for CFRP using the ECT method has been conducted. Fraunhofer Institute for Nondestructive Testing developed an integrated high-frequency ECT instrument EddyCus® MPECS (up to 100 MHz), which is particularly suitable for inspecting raw carbon fiber materials [11,12]. Jun Cheng et al. developed a high precision low-frequency ECT system with a working frequency of up to 250 kHz. The system mainly involves the small-size transmitter-receiver (T-R) type of probe, weak-signal extraction method using the lock-in amplifier, and C-scan imaging technique [13]. An advanced modelling approach is also reported for the propagation of eddy current in CFRP, which showed good agreement with experimental result [14–17]. Wuliang Yin et al.

* Corresponding author.
E-mail address: youngasever@foxmail.com (F. Cheng).

https://doi.org/10.1016/j.compositesb.2019.107460
Received 28 April 2019; Received in revised form 16 September 2019; Accepted 16 September 2019
Available online 16 September 2019

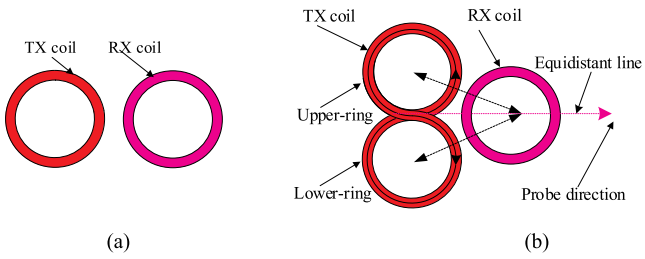

Fig. 1. (a) Schematics of the traditional T-R probe, (b) Schematics of the proposed probe.

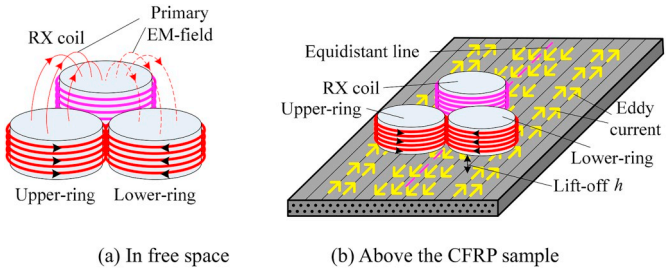

Fig. 2. Physical principle of insensitivity to lift-off.

designed multi-frequency eddy-current sensors for bulk conductivity measurements, directionality characterization, and fault detection and imaging of unidirectional, cross-ply, and impact-damaged CFRP samples [18,19]. Koichi Mizukami et al. proposed a specialized T-R probe to detect in-plane and out-of-plane fiber waviness in unidirectional CFRP by an eddy-current based nondestructive technique [20–22]. Gerhard Mook et al. developed a method to reconstruct current distribution in CFRP from the magnetic field. Delamination and impact damage were detected by rotating the probe, which consist a TX coil and a RX coil [23]. Miguel et al. presented a tailored ECT probe solution for health monitoring of highly electrically anisotropic CFRP rope at high velocity and without contact [3].

In the above studies, T-R probe is widely used to inspect the CFRP samples. The TX coil excites a primary EM-field with alternating current. The RX coil picks up the secondary EM-field, which is generated by the eddy-current and influenced by conductivity, permeability and permittivity properties of the sample. When the RX coil receives the secondary EM-field, it is unavoidable to couple the primary EM-field as background noise. Existing ECT probes are therefore more sensitive to lift-off and irregular sample surface, which may cause a larger signal than the defect and lead to defects being missed [24]. In Ref. [25], Denis Ijike Ona et al. found that both coil gap and lift-off influence probe sensitivity and proposed a solution to use driver-pick-up probe configuration to improve detection sensitivity at a given lift-off. However, these studies have not fundamentally solved the problem of lift-off effect.

Both absolute probes and traditional T-R probes are very sensitive to change due to lift-off [26]. In an ECT imaging system, there is usually a two-dimensional scanning process, with the probe scanning the CFRP plate. The roughness of the CFRP sample surface and the mechanical vibration in the scanning process will cause the probe lift-off fluctuation and reduce the signal-noise ratio of CFRP detection.

To address this problem, a new ECT probe with a special structure is proposed and applied to the detection of CFRPs. The RX coil can effectively pick up the eddy current disturbance signal caused by the properties of the CFRP sample, but is insensitive to the lift-off variation. The lift-off fluctuation will also produce a pair of common-mode signals, which can be effectively suppressed. The study provides a new means of improving the sensitivity and stability of ECT systems for CFRP materials, and similar probes have not been reported in the literature.

2. Design concept

When examining the design of probes, the point spread function (PSF) is an important consideration. The PSF of an absolute probe shows a crater shape, which indicates a low sensitivity. However, the PSF of a T-R probe assumes a Mexican hat shape with a sharp positive maximum. The spatial resolution of a T-R probe is much higher than that of an absolute probe. T-R probes with a highly focused PSF are therefore more suitable for visualizing small objects, such as carbon fiber distribution [26].

Fig. 1(b) shows the schematics of the proposed probe, which replaced circular TX coil of traditional T-R probe, as shown in Fig. 1(a), with an 8-shaped coil.

Two parts of the 8-shaped coil are referred to the upper-ring and lower-ring respectively. The RX coil is equidistant from the upper-ring and lower-ring. To facilitate the description, we define the direction of the equidistant line to be the probe direction. The proposed probe has the following characteristics: insensitivity to lift-off, characterizing fiber orientation, in-plane waviness detection, defect detection.

Fig. 2 shows the physical principle of insensitivity to lift-off. Because the RX coil is an 8-shaped coil, the primary EM-fields generated by the upper-ring and lower-ring alone the equidistant line are equal in strength and opposite in direction as shown in Fig. 2(a). The total magnetic flux excited by the 8-shape coil that penetrates the RX coil is zero, and so the output of the RX coil is also zero. The primary EM-field generated by the TX coil thus has no effect on the output of the probe.

When the probe is placed above the CFRP sample, as shown in Fig. 2 (b), with a lift-off h and the equidistant line being in the fiber orientation. Theoretically, the carbon fiber layers are separated from each other layer by a layer of matrix. However, the eddy current is not only distributed in the surface layer, but also exists in the inner layer. Cheng Jun et al. demonstrated the actual skin depth of eddy current in unidirectional CFRPs [26]. Koichi Mizukami et al. studied and simulated eddy current distribution in unidirectional CFRP [21]. Due to the anisotropy of CFRPs, conductivity varies significantly in different directions. The eddy current was mainly distributed along the fiber orientation. Fig. 2 (b) shows the eddy current distribution in a single layer at a particular moment. For unidirectional CFRP, eddy current distribution in each layer is the same, while density decreases with depth. The eddy current in a CFRP sample without defects is induced along the fiber orientation, and forms two loops with the equidistant line as the axis of symmetrical axis. The secondary EM-field induced by the eddy-current is horizontal in any lift-off above the equidistant line. The output of the RX coil is thus always zero and insensitive to the lift-off h. Therefore, to some extent, the proposed probe can overcome the interference of the vibration caused by the scanning mechanism to the output signal.

Through the above analysis, the probe direction must correspond to the fiber orientation of the CFRP sample during the scanning process. In existing methods, an auxiliary probe, which contains a TX coil and a RX coil, is rotated to identify the fiber orientation of the CFRP sample [18]. The fiber orientation can be determined when the output of the RX coil is at maximum during probe rotation. In this study, the proposed probe can be directly used to characterize fiber orientation of the CFRP sample. During the test, it requires neither the auxiliary probe nor rotating the probe and looking for the maximum. Fig. 3 shows the physical principle of characterizing fiber orientation.

Theoretically, when the probe direction agrees with the fiber orientation during the scanning process, the output of the RX coil is zero. If the fiber is right-deflected to the probe orientation (i.e., $\theta < 0°$), as shown in Fig. 3(a), the coupling between the RX coil and the upper-ring is enhanced. In this case, the RX coil will output a signal in-phase with the excitation signal. Conversely, if the fiber is left-deflected to the probe direction (i.e., $\theta > 0°$), as shown in Fig. 3(b), the phase of the RX coil signal is opposite to that of the excitation signal.

This characteristic can be applied in two ways. Firstly, the fiber

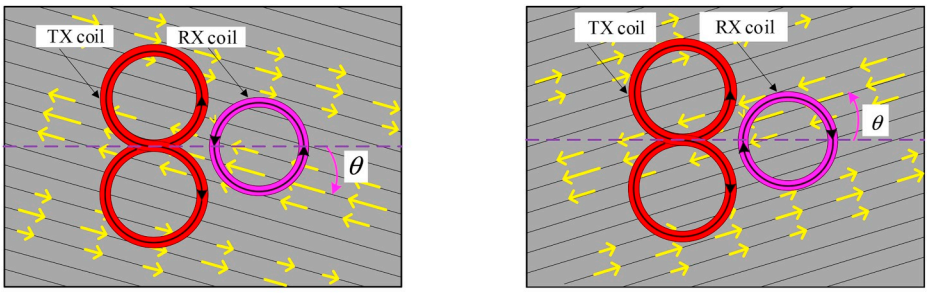

(a) With right-deflection (b) With left-deflection

Fig. 3. Physical principle of characterizing fiber orientation (top view).

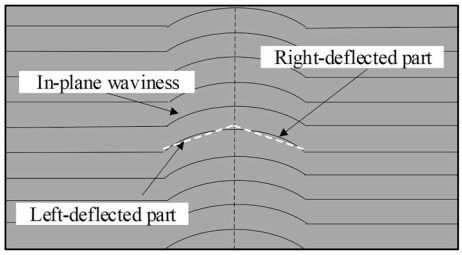

Fig. 4. Schematics of unidirectional CFRP with in-plane waviness.

orientation of the CFRP material can be characterized to check whether the fiber deviates from the original designed orientation. From the phase of the output signal, the fiber can be determined to be right-deflected (in-phase) or left-deflected (out-of-phase). Secondly, according to the amplitude and phase of the output signal, the probe can align closely to the fiber orientation to improve the sensitivity in the scanning process.

Fig. 4 shows the schematic of in-plane waviness detection. A single occurrence of in-plane waviness can be approximately regarded as the combination of a left-deflection and a right-deflection. If a CFRP sample with in-plane waviness is tested, the eddy current path is bent along the waviness. The bending eddy current path creates an imbalance of magnetic fluxes on either side of the equidistant line. When the RX coil is above the in-plane waviness zone, an induced voltage corresponding to the waviness will be generated in the RX coil. As can be seen from Fig. 5 (a), above the left-deflected part of the in-plane waviness, the RX coil will emit a signal that is out-of-phase to the excitation signal. In the situation shown in Fig. 5(b), the detection signal will be in-phase with excitation signal.

Fig. 6 shows the physical principle of defect detection with the proposed probe. If there is a defect on the left side of the equidistant line, as shown in Fig. 6(a), the eddy current on the left side will be disturbed. The eddy-current on the either side of the equidistant line will become imbalanced. The output is in-phase with the excitation signal. The opposite situation will occur if the defect is on the right side. However, if the defect is in the center of the RX coil, as shown in Fig. 6(b), the disturbed eddy-current is still symmetrical about the equidistant line. In this case, the total magnetic flux passing through the RX coil will be zero, resulting in no signal. When the defect is scanned by the probe, there is therefore a pattern of double peaks on the signal amplitude image.

From the descriptions above, we can see that the output is only related to the secondary EM-field induced by the eddy current, not to the

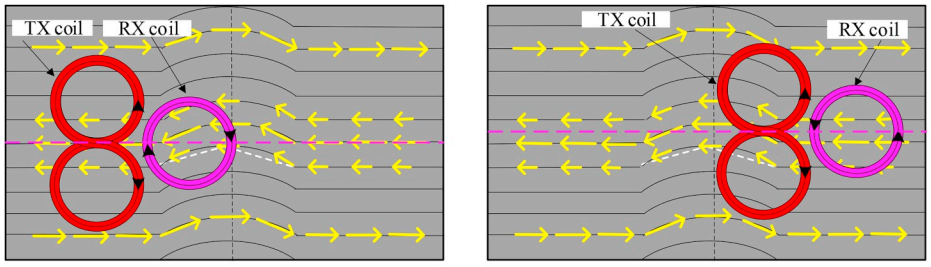

(a) Probe above left-deflected part (b) Probe above right-deflected part

Fig. 5. Physical principle of in-plane waviness detection (top view).

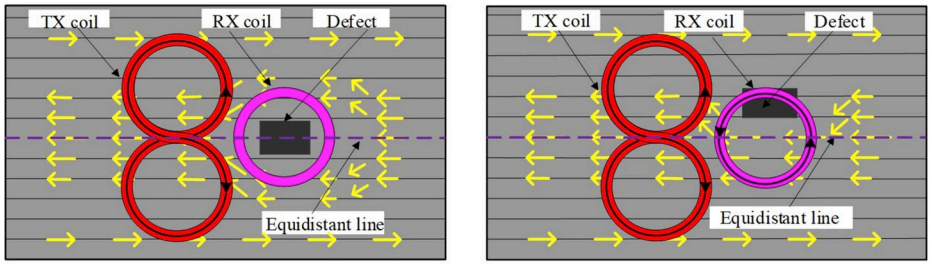

(a) Probe above left-deflected part (b) Probe above right-deflected part

Fig. 6. Physical principle of defect detection (top view).

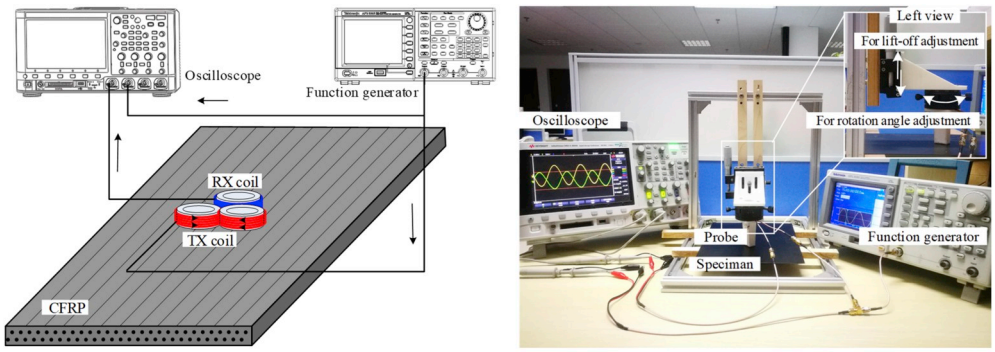

Fig. 7. Experimental setup.

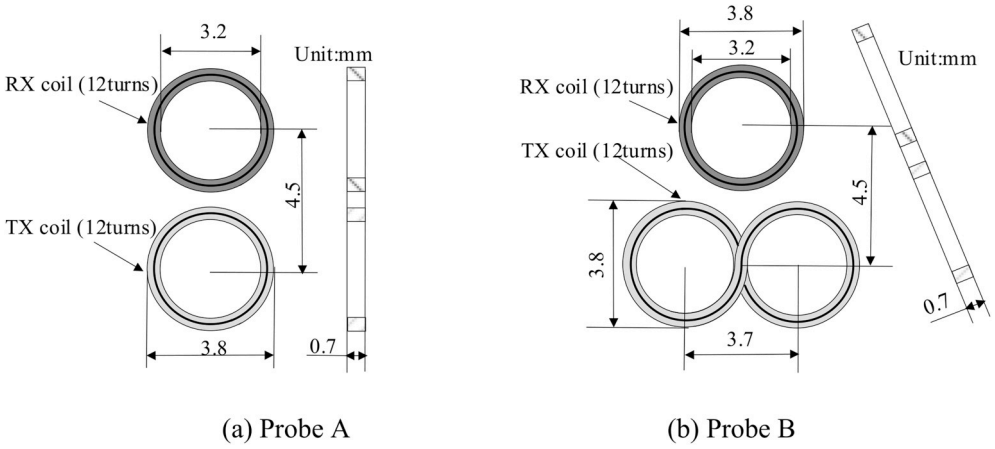

Fig. 8. Geometric parameters of experimental probes.

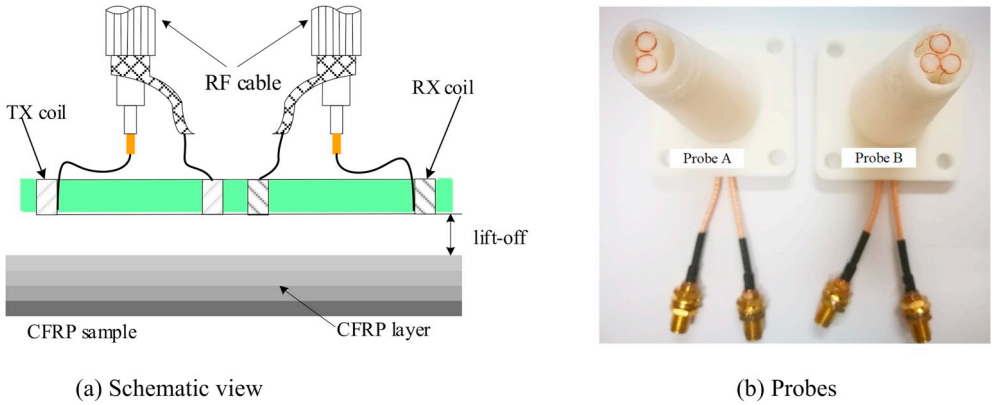

Fig. 9. ECT probes used in the experiments.

primary EM-field excited by the TX coil. This is a significant feature of the proposed probe. Although the physical principles mentioned above are analyzed on unidirectional laminates, the proposed probe still works on orthogonal woven laminates and cross-ply laminates. Subsequent experiments on these laminates verified this point.

3. Experiments and discussions

3.1. Experiments of insensitivity to lift-off

The reduction in the interferences, such as the lift-off effect in ECT systems has been difficult. The characteristic of insensitivity to lift-off is one of the merits of the proposed ECT system, which can therefore offer more accurate testing results. To validate this, an ECT experimental platform with an adjustable lift-off has been built, as shown in Fig. 7. It is comprised of a translation stage, a rotation stage, an oscilloscope, and a function generator.

A smaller sized coil can provide a more accurate estimation of the position and length of cracks. For convenience of handcrafting of the 8-shaped coil, two probes with geometric parameters shown in Fig. 8 were designed and fabricated. Probe A is a traditional T-R probe, consisting of two air-cored circular coils with 0.2 mm wire diameter and 12 turns. The two coils are the same size (3.2 mm inner diameter and 3.8 mm outer diameter) and the distance between them is 3.8 mm, as shown in Fig. 9

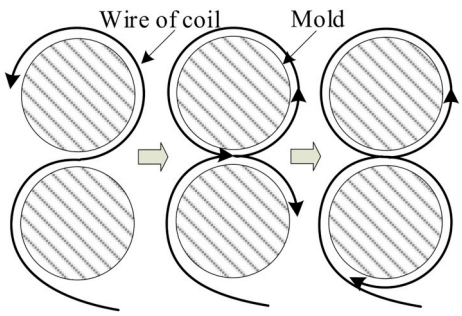

Fig. 10. Winding procedure of 8-shaped coil.

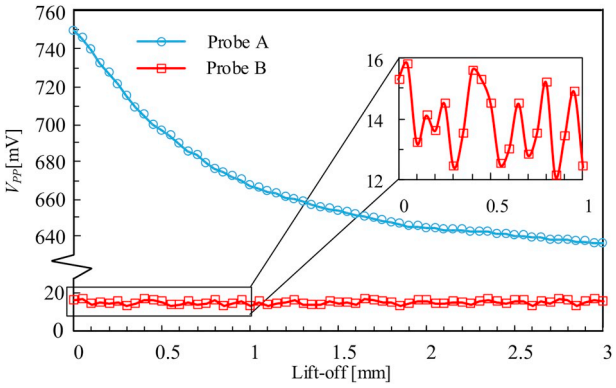

Fig. 11. Output signal variation with lift-off.

(a). Probe B is the probe proposed in this paper. The TX coil is 8-shaped with wire diameter of 0.2 mm and 12 turns. The RX coil is the same size as that of probe A, and is 4.5 mm from the center of the 8-shaped TX coil. The detailed parameters of the probes are shown in Fig. 9(b). Fig. 10 shows the method of winding the 8-shaped coil.

Firstly, a unidirectional CFRP specimen without defect was put on the stage. The Probe A was mounted on the holder. The fiber orientation and equidistant line was maintained in the same direction. An excitation signal generated from a function generator (Tektronix AFG3101) was applied to the TX coil with a peak-to peak value of 10 V at a frequency of 15 MHz. The output of the RX coil was measured using an oscilloscope (Keysight DSO-X-2024A). The lift-off was changed from 0 to 3.0 mm at interval of 0.05 mm by adjusting the translation stage. The relationship between lift-off and amplitude of output signal of is shown in Fig. 11.

The output of probe A, has an obvious downward trend with increase of lift-off. The rate of decline decreases gradually. However, the decrease in the output signal is almost linear when lift-off changes between 0 and 1.0 mm. The corresponding decrease is approximately 80 mV. For practical application, if the random variation of lift-off fluctuates between 0 and 1.0 mm, the signal noise will be approximately 80 mV. This mean variation of lift-off may mask the signal caused by small defects. Theoretically, the output of probe B should be zero. In fact, it is nonzero (but only about 14 mV), which is due to imperfect winding of the 8-shaped coil. It appears that the output signal of probe B is not affected by lift-off variation. When lift-off changes between 0 and 3.0 mm, there is no indication that the output signal varies with the increase of lift-off. The fluctuation is within 2 mV, which is much smaller compared with change of the output of probe A. This mean that a variation of lift-off caused by the scanning mechanism will not result in significant change in the output signal. The results shown in Fig. 11 show that the proposed probe is less affected by lift-off effect.

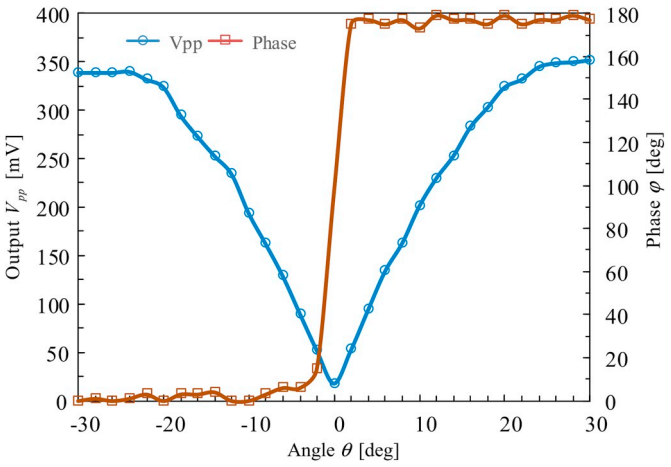

Fig. 12. Output property of the proposed probe with different angle θ on a unidirectional CFRP.

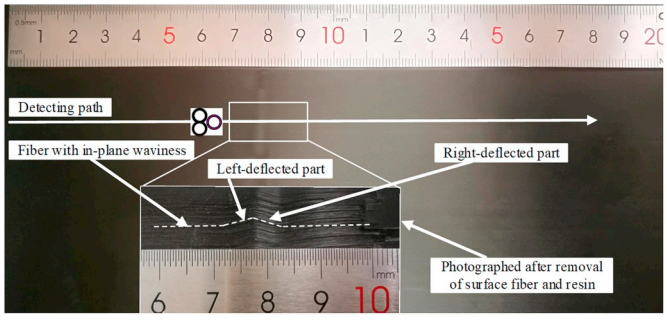

Fig. 13. Unidirectional CFRP specimen with in-plane waviness.

3.2. Experiments of characterizing fiber orientations

When the probe azimuth aligns with the fiber orientation, the output voltage is almost 0. The system is more sensitive to defects. In addition, characterization of the fiber orientation can be used for the characterization of CFRPs [18]. The specimen and experimental platform used in Section 3.1 are also used in this section. The lift-off was set to 0.5 mm and the excitation signal was a sinusoidal wave with peak to peak value of 10 V at a frequency of 15 MHz. The angle θ between probe B and the fiber orientation was adjusted from $\theta = -30°$ to $\theta = 30°$ at interval of 2°. The variation of the amplitude of the output signal V_{PP} and the phase ϕ between the excitation signal and output signal are shown in Fig. 12.

Fig. 3 shows the schematic of characterizing fiber orientation. When the probe azimuth is aligned with the fiber orientation (i.e., $\theta = 0°$), the output voltage of the pickup coil is at minimum (almost to zero). If $\theta < 0°$ (the fiber is right-deflected to the probe azimuth as shown in Fig. 3(a)), the phase ϕ is zero. Conversely, if $\theta > 0°$ (the fiber is left-deflected to the probe azimuth as shown in Fig. 3(b)), $\phi = 180°$. That is to say, the output signal is out-of-phase with the excitation signal. But the output will increase as long as the fiber direction deviates from the probe azimuth, for both $\theta < 0°$ and $\theta > 0°$. Therefore, with analysis of the variation of V_{PP} and ϕ, the fiber orientation can be determined.

3.3. Experiments of in-plane waviness detection

Fig. 13 show the specimen for in-plane waviness detection. The prepreg of the unidirectional CFRP specimen used in this experiment and cross-ply laminate used in Section 3.4 are P2255-17 (TORAY INDUSTRIES, INC, layer thickness is 0.14 mm with TORAYCA™ RESIN No.2592). There is a left-sided waviness (approximately 0.62 mm beneath the surface of the specimen) in the middle of the plate. Probe B

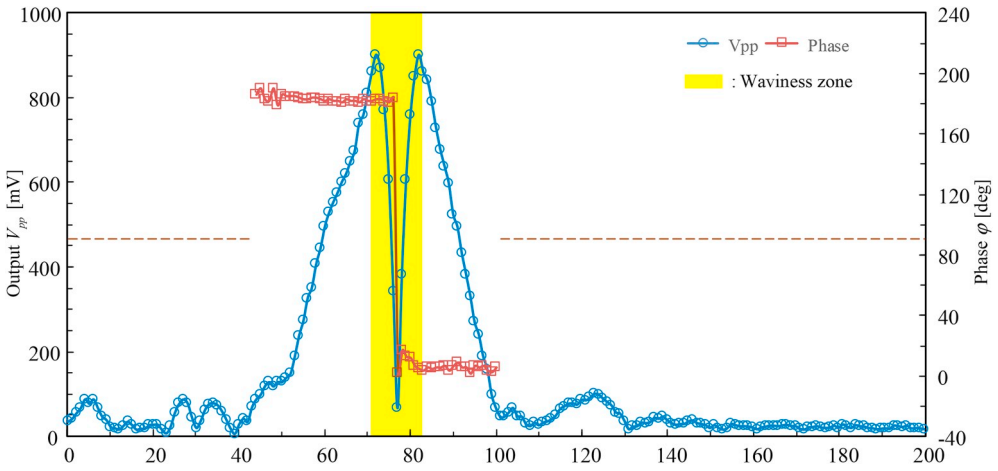

Fig. 14. Result of ECT of in-plane waviness detection.

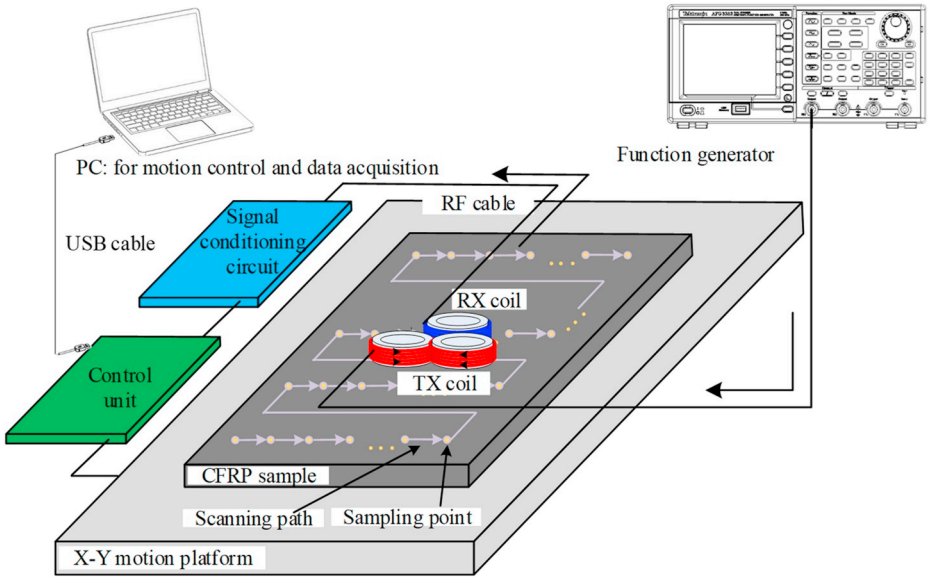

(a) Schematic view

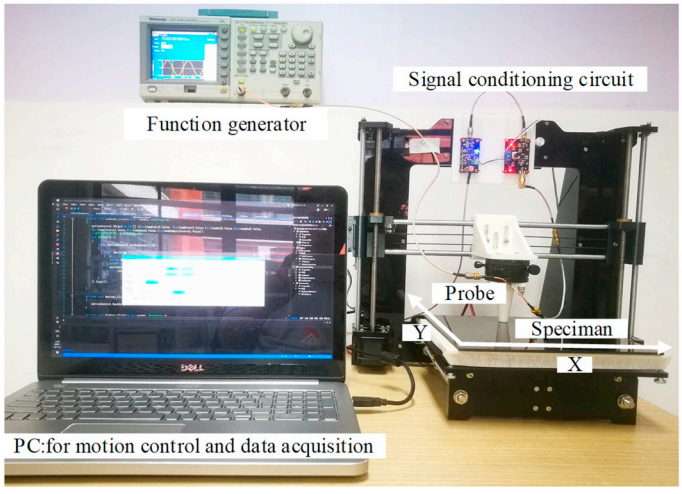

(b) Photo

Fig. 15. ECT scanning setup.

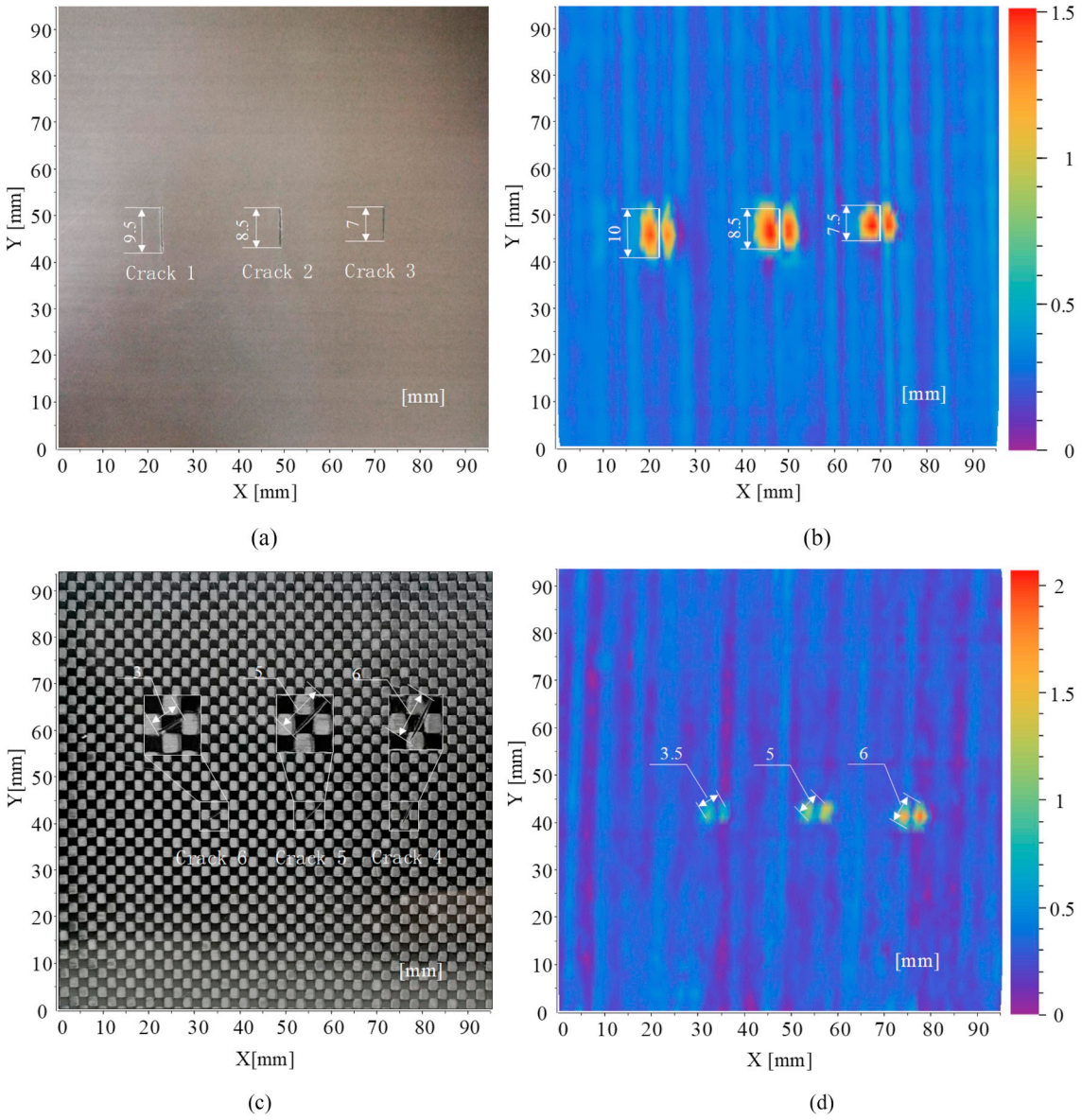

Fig. 16. the CFRP sample and the scan image.

was moved along the fiber direction at interval of 1 mm. The excitation signal is sinusoidal wave with peak-to-peak value of 10 V, and a frequency of 15 MHz. The results were obtained as shown in Fig. 14.

The output signal collected in the intact zone is almost white noise with an amplitude close to zero and an unstable phase. The waveform of the output signal displayed on the oscilloscope has no obvious periodicity. It is difficult to read the exact value of the phase due to its constant variation, so it is represented by a dotted line on the graph. In Fig. 13, it can be seen that: (1) the output signal amplitude in the figure has two peaks at 72 mm and 82 mm, respectively. (2) At 72 mm, the output signal is out-of-phase (i.e., $\phi = 180°$), while at the peak of 82 mm, the two signals are in phase (i.e., $\phi = 0°$), with the phase reversal occurring at 77 mm. Therefore, according to the experimental results, the following judgments can be made: 1) in-plane waviness exists in the tested sample, with its center located at 77 mm; 2) the waviness ranges from 72 mm to 82 mm (i.e. the yellow area in Fig. 13); 3) the shape of the waviness can be determined by the distribution of the phase angle, and the fiber between 71 mm and 77 mm being left-deflected, while the fiber between 77 mm and 82 mm being right-deflected. The experimental results are in good agreement with the actual waviness shape in the photograph after removing the surface fiber and resin, as shown in Fig. 12.

The experiment confirms that the proposed probe can not only detect in-plane waviness, but also can be used to estimate the position, range, and shape of waviness. The length of the waviness is roughly equal to the distance between the two peaks of output signal. If the waviness is left-sided, the phase of the output signal changes from out-of-phase to in-phase. Similarly, if the waviness is right-sided, the phase of output signal will change from in-phase to out-of-phase. In addition, as seen from Fig. 13, the in-plane waviness is not on the surface layer. Therefore, confirmation of in-plane waviness detection also proved that the eddy currents are not only distributed in the surface layer, which agrees well with the analysis in Section 2.

3.4. Defects scanning

Fig. 15 shows the scanning setup. The CNC X–Y scanning machine was controlled through PC-based software. Data analysis and visualization was performed in Wolfram Mathematic 11.1.

Fig. 16 shows the specimens adopted in this experiment and the

Table 1
Information about size of cracks and experimental parameters.

Specimen	Crack No.	Crack Length l (mm)	Width w (mm)	Depth d (mm)	Frequency f (MHz)	Lift-off h (mm)
cross-ply laminate	1	9.5	0.5	0.4		
	2	8.5	0.4	0.5	20	0.5
	3	7.0	0.4	0.5		
orthogonal woven laminate	4	6.0	0.4	0.4		
	5	5.0	0.3	0.3	15	0.5
	6	3.0	0.3	0.3		

corresponding scanning results. The cloth of orthogonal woven laminate is CO6644B (TORAY INDUSTRIES, INC, layer thickness is 0.3 mm). The size of cracks and experimental parameters are shown in Table 1. Probe B was installed on the bracket and the probe azimuth is in line with the Y axis.

The cracks were detected and visualized, and the areas with cracks were strongly distinguished from the surrounding area. For example, from the axis of coordinates in Fig. 16(b), the position of center of crack 1 is at approximately (23 mm, 45 mm). Its length is about 10 mm, stretching from 41 mm to 51 mm on the X axis. This is in good agreement with the specimen shown in Fig. 16(a). Moreover, there are two symmetrical peaks on the image. This agrees with the theoretical analysis of the principle of defect detection in Section 2. From Fig. 16(b) and (d), we can see the relationship of the crack length: crack 1 > crack 2 > crack3, crack 4 > crack 5 > crack 6. This agrees with the data shown in Table 1. In addition, for these 6 cracks in two specimens, the error between experimental results and the length of the actual cracks is within 1 mm. The light and dark textures in the vertical direction (Y direction) can also be observed from the scanning image shown in Fig. 15(b), which is mainly due to the uneven distribution of vertical fibers in the actual manufacturing process of CFRPs. It can be seen from Fig. 15(b) and (d) that the distribution of fiber bundles in line with the probe direction (Y in the above experiment) can be effectively detected, while the distribution of fiber bundles in the non-probe direction (e.g. X direction) will not appear on the image. This means that the proposed probe has a certain direction selectivity, which can be used to selectively detect the fiber distributed in a specific direction. This may be addressed in our further studies.

4. Conclusions

(1) A special T-R probe with an 8-shaped TX coil has been designed. The frequency range for the proposed probe is 10 MHz–25MHz without additional instruments. The probe can be used for in-plane waviness detection, defect detection and characterizing fiber orientation of CFRPs.
(2) For the proposed probe, the output is only related to the secondary EM-field induced by the eddy current, not to the primary EM-field excited by the TX coil. The probe is therefore insensitivity to lift-off and can therefore overcome the interference of mechanical vibration in the scanning process and uneven surface of CFRP sample.
(3) For in-plane waviness, the defects are reflected in the signal amplitude. The experiment shows that the proposed probe can also be used to determine the position, range and shape of waviness.
(4) According to the phase of output signal, it can be directly determined whether the fiber is left-deflected or right-deflected. Therefore, the proposed probe does not need to be rotated for a whole circle to find the fiber direction.
(5) When a defect is scanned by the proposed probe, there is a pattern of double peaks on the signal amplitude image.
(6) The probe can be used to image the CFRPs with defects, which made the test results more intuitive and realized data visualization. Defects can be clearly visualized in the scan image. This work can be applied to the development of automatic detecting system for CFRP material.

Declaration of interests

The authors declare that they have no known competing financial interests or personal relationships that could have appeared to influence the work reported in this paper.

Acknowledgement

This work was supported by National Natural Science Foundation of China (51677158).

Appendix A. Supplementary data

Supplementary data to this article can be found online at https://doi.org/10.1016/j.compositesb.2019.107460.

References

[1] Beardmore P, Johnson CF. The potential for composites IN structural automotive applications. Compos Sci Technol 1986;26(4):251–81.
[2] Cheng J, Qiu J, Xu X, Ji H, Takagi T, Uchimoto T. Research advances in eddy current testing for maintenance of carbon fiber reinforced plastic composites. Int J Appl Electromagn Mech 2016;51(3):261–84.
[3] Machado MA, Antin K-N, Rosado LS, Vilaca P, Santos TG. Contactless high-speed eddy current inspection of unidirectional carbon fiber reinforced polymer. Compos B Eng 2019;168:226–35.
[4] Caminero MA, Garcia-Moreno I, Rodriguez GP, Chacon JM. Internal damage evaluation of composite structures using phased array ultrasonic technique: impact damage assessment in CFRP and 3D printed reinforced composites. Compos B Eng 2019;165:131–42.
[5] Rolfe E, Kelly M, Arora H, Hooper PA, Dear JP. Failure analysis using X-ray computed tomography of composite sandwich panels subjected to full-scale blast loading. Compos B Eng 2017;129:26–40.
[6] Kolanu NR, Raju G, Ramji M. Damage assessment studies in CFRP composite laminate with cut-out subjected to in-plane shear loading. Compos B Eng 2019;166:257–71.
[7] Dua G, Mulaveesala R, Kher V, Rani A. Gaussian windowed frequency modulated thermal wave imaging for non-destructive testing and evaluation of carbon fibre reinforced polymers. Infrared Phys Technol 2019;98:125–31.
[8] Arora V, Mulaveesala R. Application of golay complementary coded excitation schemes for non-destructive testing of sandwich structures. Opt Lasers Eng 2017;93:36–9.
[9] He Y, Chen S, Zhou D, Huang S, Wang P. Shared excitation based nonlinear ultrasound and vibrothermography testing for CFRP barely visible impact damage inspection. IEEE Trans Ind Inf 2018;14(12):5575–84.
[10] He Y, Yang R, Zhang H, Zhou D, Wang G. Volume or inside heating thermography using electromagnetic excitation for advanced composite materials. Int J Therm Sci 2017;111:41–9.
[11] Heuer H, Schulze M. Eddy current testing of carbon fiber materials by high resolution directional sensors. Int Workshop Smart Mater Struct NDT Aero Montreal 2011 p. 1-10.
[12] Schulze MH, Heuer H. Textural analyses of carbon fiber materials by 2D-FFT of complex images obtained by high frequency eddy current imaging (HF-ECI). In: Gyekenyesi AL, Yu TY, Shull PJ, Diaz AA, Wu HF, editors. Nondestructive characterization for composite materials, aerospace engineering, civil infrastructure, and homeland security; 2012. 2012.
[13] He YZ, Tian GY, Pan MC, Chen DX. Non-destructive testing of low-energy impact in CFRP laminates and interior defects in honeycomb sandwich using scanning pulsed eddy current. Compos B Eng 2014;59:196–203.
[14] Cheng J, Ji H, Qiu J, Takagi T, Uchimoto T, Hu N. Novel electromagnetic modeling approach of carbon fiber-reinforced polymer laminate for calculation of eddy currents and eddy current testing signals. J Compos Mater 2015;49(5):617–31.
[15] Mizukami K, Mizutani Y, Todoroki A, Suzuki Y. Analytical solutions to eddy current in carbon fiber-reinforced composites induced by line current. Adv Compos Mater 2016;25(4):385–401.
[16] Jiao S, Li J, Du F, Sun L, Zeng Z. Characteristics of eddy current distribution in carbon fiber reinforced polymer. J Sens 2016.
[17] Rezgui S, Mohellebi H, Feliachi M. Electromagnetic modeling of carbon-fiber reinforced composite materials using the wave digital concept. Multidimens Syst Signal Process 2018;29(1):405–30.
[18] Yin WL, Withers PJ, Sharma U, Peyton AJ. Noncontact characterization of carbon-fiber-reinforced plastics using multifrequency eddy current sensors. IEEE Trans Instrum Meas 2009;58(3):738–43.

[19] Yin W, Li X, Withers PJ, Peyton AJ. Non-contact characterization of hybrid aluminium/carbon-fibre-reinforced plastic sheets using multi-frequency eddy-current sensors. Meas Sci Technol 2010;21(10).
[20] Mizukami K, Mizutani Y, Kimura K, Sato A, Suzuki Y, Nakamura Y. Visualization and size estimation of fiber waviness in multidirectional CFRP laminates using eddy current imaging. Compos Appl Sci Manuf 2016;90:261–70.
[21] Mizukami K, Mizutani Y, Todoroki A, Suzuki Y. Detection of in-plane and out-of-plane fiber waviness in unidirectional carbon fiber reinforced composites using eddy current testing. Compos B Eng 2016;86:84–94.
[22] Mizukami K, Mizutani Y, Kimura K, Sato A, Todoroki A, Suzuki Y. Detection of in-plane fiber waviness in cross-ply CFRP laminates using layer selectable eddy current method. Compos Appl Sci Manuf 2016;82:108–18.
[23] Mook G, Lange R, Koeser O. Non-destructive characterisation of carbon-fibre-reinforced plastics by means of eddy-currents. Compos Sci Technol 2001;61(6):865–73.
[24] Fu YW, Lei ML, Li ZX, Gu ZT, Yang H, Cao AS, et al. Lift-off effect reduction based on the dynamic trajectories of the received signal fast Fourier transform in pulsed eddy current testing. NDT E Int 2017;87:85–92.
[25] Ona DI, Tian GY, Sutthaweekul R, Naqvi SM. Design and optimisation of mutual inductance based pulsed eddy current probe. Measurement 2019;144:402–9.
[26] Cheng J, Qiu JH, Ji HL, Wang ER, Takagi T, Uchimoto T. Application of low frequency ECT method in noncontact detection and visualization of CFRP material. Compos B Eng 2017;110:141–52.